No. 220
July 1979

A Contribution to Flow-Separation Problem in Unsteady Motion of a Body

Yoji Himeno

This research was carried out in part
under the Naval Sea Systems Command
General Hydrodynamics Research Program,
Subproject SR 009 01 01, administrated by the
Naval Ship Research and Development Center
Contract No. N00014-79-C-0244

It was also supported by the
Japan Shipbuilding Industry Foundation

Department of Naval Architecture
and Marine Engineering
College of Engineering
The University of Michigan
Ann Arbor, Michigan 48109

REPORT DOCUMENTATION PAGE		READ INSTRUCTIONS BEFORE COMPLETING FORM
1. REPORT NUMBER 220	2. GOVT ACCESSION NO.	3. RECIPIENT'S CATALOG NUMBER
4. TITLE (and Subtitle) A Contribution to Flow-Separation Problem in Unsteady Motion of a Body		5. TYPE OF REPORT & PERIOD COVERED Final 6. PERFORMING ORG. REPORT NUMBER 220
7. AUTHOR(s) Yoji Himeno		8. CONTRACT OR GRANT NUMBER(s) N00014-79-C-0244
9. PERFORMING ORGANIZATION NAME AND ADDRESS Dept. of Naval Arch & Mar Engr The University of Michigan Ann Arbor, MI 48109		10. PROGRAM ELEMENT, PROJECT, TASK AREA & WORK UNIT NUMBERS 61153N R02301 SR 023 01 01
11. CONTROLLING OFFICE NAME AND ADDRESS David W. Taylor Naval Ship R&D Center (1505) Bethesda, MD 20084		12. REPORT DATE July 1979 13. NUMBER OF PAGES 35 + iii
14. MONITORING AGENCY NAME & ADDRESS(if different from Controlling Office) Office of Naval Research 800 N. Quincy St. Arlington, VA 22217		15. SECURITY CLASS. (of this report) UNCLASSIFIED 15a. DECLASSIFICATION/DOWNGRADING SCHEDULE

16. DISTRIBUTION STATEMENT (of this Report)

APPROVED FOR PUBLIC RELEASE: DISTRIBUTION UNLIMITED

17. DISTRIBUTION STATEMENT (of the abstract entered in Block 20, if different from Report)

18. SUPPLEMENTARY NOTES

Sponsored by the Naval Sea Systems Command General Hydromechanics Research (GHR) Program administered by the David W. Taylor Naval Ship R&D Center, Code 1505, Bethesda, MD 20084.

19. KEY WORDS (Continue on reverse side if necessary and identify by block number)

SHIP MOTIONS
ROLL DAMPING
SEPARATION

20. ABSTRACT (Continue on reverse side if necessary and identify by block number)

Roll motion is the least predictable of ship motions, largely because of viscosity effects, which in turn causes flow separations to occur. As a result of these phenomena, roll damping is often highly nonlinear. It is best estimated in the present state of the art by strictly empirical methods.

In this report, several relevant flow-separation problems are studied from a fundamental point of view. These are divided gener-

ally into two categories: (i) boundary-layer separation and (ii) sharp-edge separation. In both cases, starting motion and oscillatory motion are considered separately. Emphasis is placed on rather simple methods of calculations. Results are compared with experiments and/or more detailed calculation methods wherever such are available. Finally, a procedure is proposed (but not carried out) for treating the formation of vortex sheets by a translating rolling ship hull.

ABSTRACT

Roll motion is the least predictable of ship motions, largely because of viscosity effects, which in turn causes flow separations to occur. As a result of these phenomena, roll damping is often highly nonlinear. It is best estimated in the present state of the art by strictly empirical methods.

In this report, several relevant flow-separation problems are studied from a fundamental point of view. These are divided generally into two categories: (i) boundary-layer separation and (ii) sharp-edge separation. In both cases, starting motion and oscillatory motion are considered separately. Emphasis is placed on rather simple methods of calculations. Results are compared with experiments and/or more detailed calculation methods wherever such are available. Finally, a procedure is proposed (but not carried out) for treating the formation of vortex sheets by a translating rolling ship hull.

CONTENTS

1. INTRODUCTION

The prediction of hydrodynamic forces on an oscillating ship hull is now one of the most important problems of ship hydrodynamics. Among several factors affecting the forces, the one due to fluid viscosity is still left for theoretical treatment. One of the reasons seems to be the difficulty of treating the separating flow around a bluff body like a ship hull.

There are several features of flow separation around a ship hull. In the absence of ship speed, the separation occurs at the stem and the stern, forming vertical vortices during lateral ship motions. Bilge separation also occurs, shedding horizontal vortices near the turn of the bilge if the radius of the bilge circle is small enough. When the ship moves forward, these vortices flow downstream, forming a vortex wake which is oscillating and mixing into the ship wake caused by the steady forward motion. At present, it is impossible to handle all of these complicated vortex features in a single system. Some sort of simplification is necessary to treat them.

In this paper, several attempts are made to predict flow separation around an oscillating ship hull. In the case of zero ship speed, the problem is reduced to two-dimensional flow separation, which can be treated in two ways. One is the separation from a smooth curved surface, which is discussed in Chapter 2. The other is the separation at a sharp edge or corner. The most simplified case of the latter, *viz.*, the flat-plate case, is treated in Chapter 3 by a simple approach. In Chapter 4, a method is proposed for obtaining hydrodynamic forces on an oscillating ship hull with and/or without forward speed, in which the flow is described in terms of vortex sheets shedding from the separation points on the hull. A numerical calculation scheme for the vortex-sheet formation is stated. However, the computation is not completed, partly because of the difficulty of avoiding the self-mixing and the instability of the vortex sheet in an oscillatory motion, which is also discussed in Chapter 4.

2. BOUNDARY-LAYER SEPARATION

In order to consider the separation problem in oscillatory motion, it is easier to begin the analysis with a starting motion. The motion starts from rest with an acceleration in one direction and then ceases with a deceleration in the opposite direction. This might roughly correspond to an arbitrary single swing during an oscillation period.

After the discussion of this starting motion in Section 2.1, the analysis of oscillating motion according to Schlichting's solution will be made in Section 2.2.

2.1 Flow Separation in Starting Motion

For any arbitrary shape of body without sharp-edge corners, the separation point can be determined by boundary-layer theory. Suppose the velocity at the outer edge of the boundary layer, $U(x,t)$, is given in the form

$$\left.\begin{aligned} U(x,t) &= 0 && t \le 0 , \\ &= U_0(x)(t+\beta t^3) , && t \ge 0 , \end{aligned}\right\} \qquad (2.1)$$

where x is measured from the front stagnation point along the surface of the body, and t represents time. The coefficient β represents an additional acceleration ($\beta>0$) or deceleration ($\beta < 0$). Without the β term, the flow would correspond to the case of a starting motion with constant acceleration, which was treated by Blasius [1]. The objective of this section is to extend Blasius' treatment to the case with an additional deceleration term ($\beta < 0$).

The solution can be obtained by an expansion in time series. Suppose the stream function $\psi(x,y,t)$ is expanded in the form

$$\psi(x,y,t) = 2\sqrt{\nu t}\{U\zeta_0 + tU\frac{\partial U}{\partial x}\zeta_1 + \ldots\}$$

$$= 2\sqrt{\nu t}\{U_0 t\zeta_0 + t^3(U_0\beta\zeta_0 + U_0\frac{dU_0}{dx}\zeta_1 + \ldots)\} \quad , \quad (2.2)$$

where y is measured normal to the wall, ν is the kinematic viscosity, and the quantities $\zeta_0, \zeta_1, \ldots$ are functions of a normalized coordinate $\eta \equiv y/2\sqrt{\nu t}$. Then the velocity components u and v with respect to x and y are expressed in the form

$$\left.\begin{aligned} u &= \frac{\partial\psi}{\partial y} = U(\zeta_0' + t\frac{\partial U}{\partial x}\zeta_1' + \ldots) \quad , \\ v &= -\frac{\partial\psi}{\partial x} = -2\sqrt{\nu t}\left\{\frac{\partial U}{\partial x}\zeta_0 + t\zeta_1\{(\frac{\partial U}{\partial x})^2 + U\frac{\partial^2 U}{\partial x^2}\} + \ldots\right\} \quad . \end{aligned}\right\} \quad (2.3)$$

The present governing equation is the boundary-layer equation for unsteady motion, which can be written in the form

$$\frac{\partial u}{\partial t} + u\frac{\partial u}{\partial x} + v\frac{\partial u}{\partial y} - U\frac{\partial U}{\partial x} - \frac{\partial U}{\partial t} - \nu\frac{\partial^2 u}{\partial y^2} = 0 \quad , \quad (2.4)$$

with the boundary conditions

$$\left.\begin{aligned} u = v &= 0 \quad \text{at} \quad \eta = 0 \quad , \\ u &= U \quad \text{at} \quad \eta = \infty \quad . \end{aligned}\right\} \quad (2.5)$$

Substituting u and v into Eq. (2.4) and noting that

$$(\frac{\partial}{\partial t})_{y=\text{const.}} = (\frac{\partial}{\partial t})_{\eta=\text{const.}} - \frac{\eta}{2t}\frac{\partial}{\partial\eta} \quad ,$$

we can obtain the following time series:

$$U_0(\zeta_0' - \frac{\eta}{2}\zeta_0'' - 1 - \frac{1}{4}\zeta_0''') + U_0 t^2\{U_0'(3\zeta_1' - \frac{\eta}{2}\zeta_1'' - \frac{1}{4}\zeta_1''' - 1 + \zeta_0'^2 + \zeta_0\zeta_0'') + \beta(3\zeta_0' - \frac{\eta}{2}\zeta_0'' - \frac{1}{4}\zeta_0''' - 3)\} + \ldots = 0 \quad . \quad (2.6)$$

The equation of the first-order solution ζ_0 is as follows:

$$\zeta_0''' + 2\eta\zeta_0'' - 4\zeta_0' = -4 \quad , \quad (2.7)$$

with the boundary conditions

$$\zeta_0(0) = \zeta_0'(0) = 0 \quad \text{and} \quad \zeta_0'(\infty) = 1 \quad .$$

The solution was given by Blasius in terms of the velocity profile, ζ_0' :

$$\zeta_0' = 1 + \frac{2}{\sqrt{\pi}}\eta\, e^{-\eta^2} - (1+2\eta^2)\ \mathrm{erfc}\ (\eta)\ , \qquad (2.8)$$

where

$$\mathrm{erfc}\ (\eta) = 1 - \frac{2}{\sqrt{\pi}} \int_0^{\eta} \exp\ (-\eta'^2)\ d\eta'.$$

The second derivative of ζ_0 at the wall, which corresponds to the skin friction stress, has the value $\zeta_0''(0) = 4/\sqrt{\pi}$.

The second-order equation can also be derived by rearranging Eq. (2.6) and defining $\gamma = 8\beta/U_0'$:

$$\zeta_1''' + 2\eta\,\zeta_1'' - 12\zeta_1' = -4 + 4(\zeta_0'^2 + \zeta_0\zeta_0'') + \gamma(-1+\zeta_0')\ , \qquad (2.9)$$

in which the boundary conditions are homogeneous. Eq. (2.9) can be solved by dividing the quantity ζ_1 into two terms:

$$\zeta_1 = \zeta_{11} + \gamma\zeta_{12}\ . \qquad (2.10)$$

The solution for the first term, ζ_{11} , is the same as the Blasius second-order solution, which gives the value ζ_{11}'' at the wall

$$\zeta_{11}''(0) = \frac{1}{\sqrt{\pi}}\left(\frac{31}{15} - \frac{256}{225\pi}\right)\ . \qquad (2.11)$$

The equation for ζ_{12} can be expressed in the form

$$\zeta_{12}''' + 2\eta\,\zeta_{12}'' - 12\zeta_{12}' = -1 + \zeta_0'\ , \qquad (2.12)$$

with

$$\zeta_{12}(0) = \zeta_{12}'(0) = \zeta_{12}'(\infty) = 0\ .$$

This is newly obtained here and its solution can be written:

$$\zeta_{12}' = \frac{1}{\sqrt{\pi}}\, e^{-\eta^2}\left(\frac{3}{10}\eta + \frac{7}{15}\eta^3 + \frac{1}{15}\eta^5\right) - \mathrm{erfc}\ (\eta)\left(\frac{1}{2}\eta^2 + \frac{1}{2}\eta^4 + \frac{1}{15}\eta^6\right)\ , \qquad (2.13)$$

and

$$\zeta_{12}''(0) = 3/10\sqrt{\pi}\ . \qquad (2.14)$$

Summing up all of these solutions, we obtain the velocity profile in the boundary layer:

$$u = U_0 t\left[\zeta_0' + t^2\{\frac{dU_0}{dx}\zeta_{11}' + \beta(\zeta_0' + 8\zeta_{12}')\} + \ldots\right] . \qquad (2.15)$$

The skin friction stress, τ_w, is defined by the equation

$$\tau_w = \rho\nu\left.\frac{\partial u}{\partial y}\right|_{y=0} . \qquad (2.16)$$

The separation point can be found by putting $\tau_w = 0$ in Eq. (2.16), so that the condition of separation is expressed as follows:

$$1 + t^2(0.427\,\frac{dU_0}{dx} + \frac{8}{5}\beta) = 0 . \qquad (2.17)$$

Blasius' original solution contained only the first two terms in (2.17); the β term is new here. Eq. (2.17) can be interpreted as determining the separation *time* at the point where the velocity gradient dU_0/dx and the deceleration rate β are prescribed. Another interpretation is that it gives the *location* of the separation point where Eq. (2.17) is satisfied. It can be said from Eq. (2.17) that the separation occurs when the pressure gradient becomes adverse, and that the deceleration ($\beta < 0$) makes the separation occur earlier in time or further upstream in space, since a negative value of β corresponds to an adverse pressure gradient ($dU_0/dx < 0$).

We can apply this result to a couple of cases. First, consider a circular cylinder of radius R oscillating with amplitude X and frequency ω. The outer-edge velocity $U(x,t)$ of the boundary layer is given by potential-flow theory:

$$U = 2X\omega \sin\frac{x}{R}\sin\omega t . \qquad (2.18)$$

If we assume that this is a starting motion, then we obtain, by equating (2.1) and (2.18),

$$\left.\begin{aligned} U_0 &= 2X\omega^2 \sin\frac{x}{R} , \\ \beta &= -\beta_0\omega^2 . \end{aligned}\right\} \qquad (2.19)$$

The deceleration constant β_0 can be obtained by applying the least-squares method over a swing of the motion, which gives:

$$\beta_0 \simeq 1/8.8 \ . \tag{2.20}$$

Substituting Eq. (2.18) into (2.17), we can obtain the separation point x_s at an arbitrary time instant. For example, at the time $t = \pi/2\omega$, when the velocity of the cylinder is maximum, we obtain the separation-point angle θ_s measured from the top of the cylinder

$$\sin \theta_s = 0.822/K_C \ , \tag{2.21}$$

where K_C is the Keulegan-Carpenter number, $\pi X/R$, and $\theta_s = x_s/R - \pi/2$.

Eq. (2.21) shows that the separation depends on the amplitude of the motion but not on Reynolds number or frequency, according to the present analysis. However, the value of the coefficient in Eq. (2.21) is somewhat small compared with the experimental value of Ikeda *et al.* [2], as shown in Fig. 2.1. The experimental data seem to be expressed as

$$\sin \theta_s = 1.49/K_C \ . \tag{2.22}$$

We can also apply the present result, Eq. (2.17), to the case of a flat plate oscillating in its plane, if we assume that $dU_0/dx \equiv 0$ everywhere on the plate. From (2.17) and the approximation (2.20), we find that $\tau_w = 0$ when

$$\omega t = 2.345 \ . \tag{2.23}$$

In this case, the condition $\tau_w = 0$ does not indicate separation but merely the turning point of the τ_w oscillation. Details will be discussed in the next section. The value in (2.23) is in quite good agreement with the exact solution by Stokes [1]:

$$\omega t = \frac{3}{4}\pi \simeq 2.355 \ . \tag{2.24}$$

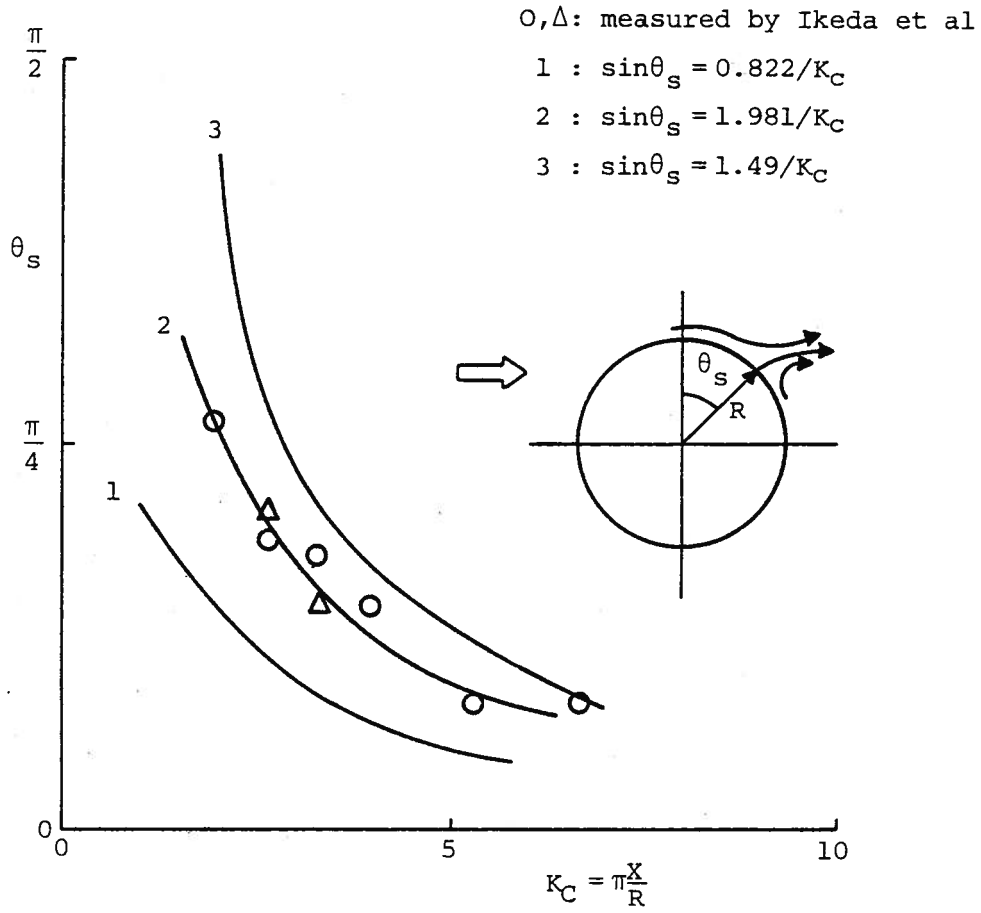

Figure 2-1. Separation angle at $t=\pi/2\omega$ for oscillating circular cylinder

This corresponds to the phase lead, $\pi/4$, of the skin friction with respect to the velocity of the body, which means that the body will experience not only a damping force but also an added-mass force due to the fluid-viscosity effect, although the phase is independent of viscosity.

Through the present analysis, it can be concluded that the flow deceleration makes the separation point move upstream and it makes the separation occur at earlier time. For the case of periodic oscillation, it corresponds to a phase lead of the flow pattern with respect to the velocity of the body.

2.2 Flow Separation in Oscillatory Motion

In the preceding section, we have discussed the starting motion by expanding the equation in time series. Therefore the results should be valid only in a small time period, and its application to oscillatory flow is also restricted within a small period of the oscillation, *i.e.*, high frequency, or small displacement of the body.

It is interesting to recall here Schlichting's approach [1] to the periodic-oscillation problem of the boundary-layer equation. After following his procedure, we shall discuss the separation condition.

The expansion is based on the assumptions

$$U \frac{\partial U}{\partial x} \Big/ \frac{\partial U}{\partial t} \propto U_{max}/\omega D \propto X/D << 1 , \tag{2.25}$$

where X is the amplitude of oscillation and D is the reference dimension of the body. Thus this is basically a small-amplitude expansion. Suppose the velocity $U(x,t)$ outside the boundary layer (the "edge velocity") is expressed in the form

$$U(x,t) = \bar{U}(x)\, e^{i\omega t} . \tag{2.26}$$

Expanding the velocity u in the boundary layer in the series

$$u = u_0(x,y,t) + u_1(x,y,t) + \dots , \tag{2.27}$$

putting this into the boundary-layer equation, (2.4), and applying the assumption (2.25), we can obtain the equations for u_0 and u_1 :

$$\frac{\partial u_0}{\partial t} - \nu \frac{\partial^2 u_0}{\partial y^2} = \frac{\partial U}{\partial t} \quad , \tag{2.28}$$

$$\frac{\partial u_1}{\partial t} - \nu \frac{\partial^2 u_1}{\partial y^2} = U \frac{\partial U}{\partial x} - u_0 \frac{\partial u_0}{\partial x} - v_0 \frac{\partial u_0}{\partial y} \quad , \tag{2.29}$$

with the usual boundary conditions.

The solutions of Eqs. (2.28) and (2.29) were given by Schlichting in the form

$$u_0 = \bar{U} e^{i\omega t}\{1 - e^{-(1+i)\eta}\} \quad , \tag{2.30}$$

$$u_1 = u_{10} + u_{11} \quad , \tag{2.31}$$

$$u_{10} = \frac{\bar{U}\bar{U}'}{\omega}\left\{-\frac{3}{4} + \frac{e^{-2\eta}}{4} + e^{-\eta}\left(\frac{1}{2}\cos\eta + 2\sin\eta\right) + \frac{\eta}{2} e^{-\eta}(\sin\eta - \cos\eta)\right\} \quad , \tag{2.32}$$

$$u_{11} = \frac{\bar{U}\bar{U}'}{\omega} e^{2i\omega t}\left\{-\frac{i}{2} e^{-(1+i)\sqrt{2}\eta} + \left(\frac{i}{2} + \frac{1-i}{2}\eta\right) e^{-(1+i)\eta}\right\} \quad , \tag{2.33}$$

where $\eta = y\sqrt{\omega/2\nu}$ and $\bar{U}' = d\bar{U}/dx$. (2.34)

The most important feature of these solutions is that there appear (i) a steady flow in Eq. (2.32) and (ii) a second-harmonic term in Eq. (2.33), both due to higher-order effects of the oscillation.

Now we have to pay attention to the skin friction variation on the wall, which leads to the condition of separation. The skin friction τ_w can be expressed in the form

$$\tau_w = \rho\sqrt{\nu\omega}\,\bar{U}\left(e^{i(\omega t+\pi/4)} + \frac{\bar{U}'}{\sqrt{2}\omega}\left\{\frac{1}{2} + (\sqrt{2}-1)e^{i(2\omega t-\pi/4)}\right\}\right) . \tag{2.35}$$

For convenience in comparing this to the result of the previous section, suppose the edge velocity is prescribed in the form

$$U = \bar{U}\sin\omega t \quad . \tag{2.36}$$

Then the skin friction can be written as follows:

$$\tau_w = \rho\sqrt{\nu\omega}\,\bar{U}\left[\sin\left(\omega t+\frac{\pi}{4}\right) + \frac{\bar{U}'}{\sqrt{2}\omega}\left\{\frac{1}{2}-(\sqrt{2}-1)\sin\left(2\omega t+\frac{\pi}{4}\right)\right\}\right] . \quad (2.37)$$

The first term coincides with that of flat-plate oscillation, while the second term, which is always positive, represents the modification of the pressure gradient or of the amplitude gradients of the external flow along the wall.

Putting $\tau_w = 0$ into Eq. (2.37), we can derive the separation condition:

$$-\frac{1}{\omega}\frac{d\bar{U}}{dx} = \frac{\sqrt{2}\sin(\omega t+\pi/4)}{1/2-(\sqrt{2}-1)\sin(2\omega t+\pi/4)} . \quad (2.38)$$

Eq. (2.38) shows that the separation occurs when and where the value of the left-hand side exceeds that of the right-hand side in one swing. The nature of the separation condition is almost the same as in the previous section in that it mainly depends on the amplitude of the motion but not on the frequency or on Reynolds number.

We can also apply Eq. (2.38) to the sway motion of a circular cylinder of radius R. From Eq. (2.18) and Eq. (2.36), the velocity amplitude is expressed as

$$\bar{U} = 2X\omega\sin x/R . \quad (2.39)$$

Let us consider again the problem of obtaining the separation point x_s or the angle $\theta_s = x_s/R - \pi/2$ at the instant $\omega t = \pi/2$. Substituting Eq. (2.39) and $\omega t = \pi/2$ into Eq. (2.28), we obtain

$$\sin\theta_s = \frac{1.981}{K_C} \qquad (K_C = \pi X/R) . \quad (2.40)$$

Eq. (2.40) has the same form as Eq. (2.21), but the coefficient differs much. The experimental value in Eq. (2.22) is almost the average of Eqs. (2.21) and (2.40), as shown in Fig. 2.1.

Fig. 2-2 shows the comparison of the separation condition in an arbitrary time within one swing. The values from Eq. (2.38) and

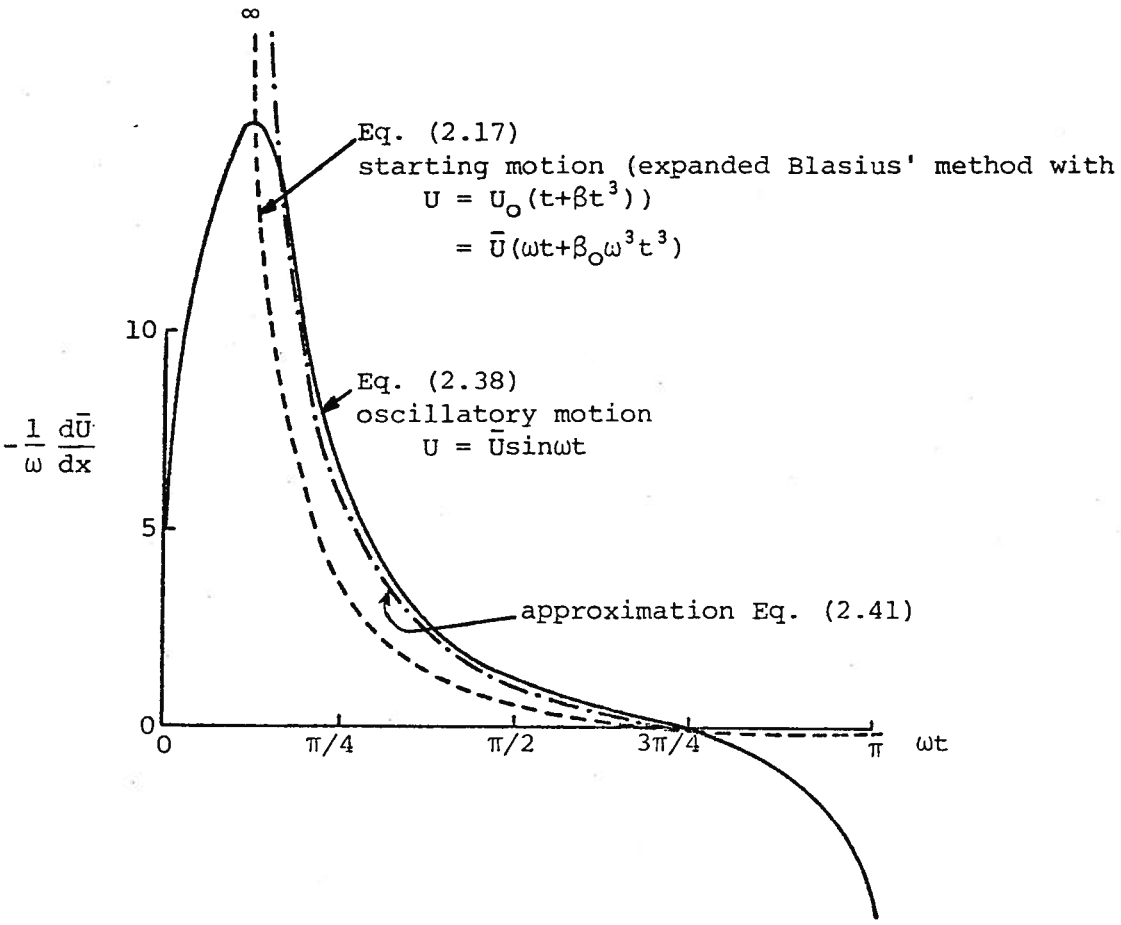

Figure 2-2. Condition of separation in one swing

and from an equation derived from (2.17) have a similar tendency in the middle part of the one-swing period. However, at both ends of the period there is a difference due to the time-history effect.

Moreover, an interesting thing is that both curves go to zero at $\omega t \simeq 3\pi/4$. This means that at this time the skin friction becomes zero at the point where $d\bar{U}/dx = 0$. In the case of a flat plate, τ_w changes its sign at $\omega t = 3\pi/4$, while in the case of a

body with round bluff corner the separation point moves upstream into the accelerated flow region ($d\bar{U}/dx > 0$) on the body surface.

Fig. 2-2 also shows an approximation curve which is determined in such a way that it agrees with the experiment at the time $\omega t = \pi/2$, *i.e.*, Eq. (2.22). The form of the curve is expressed as follows:

$$-\frac{1}{\omega}\frac{d\bar{U}}{dx} = 4.213\left\{\frac{1}{\omega^2 t^2} - \frac{16}{9\pi^2}\right\} . \tag{2.41}$$

Eq. (2.41) would be useful to obtain the separation point of an arbitrarily shaped body at any instant of one swing period.

Throughout the preceding analysis, we have considered that the separation is expressed by the condition $\tau_w = 0$. However, this condition may also imply attachment or a simple turning of τ_w without separation of the flow. An additional condition to distinguish separation from the others can be found in the following way.

Suppose the stream function $\psi(x,y,t)$ close to the wall is expanded in the form

$$\psi(x,y,t) = ay^2 + by^3 + \dots . \tag{2.42}$$

The coefficient a can be related to the skin friction τ_w , and the other coefficient, b , can also be found from the leading-order term of the boundary-layer equation, (2.4), expanded near the wall. Then Eq. (2.42) becomes

$$\psi = \frac{y^2}{2\rho\nu}\left\{\tau_w - \frac{\rho}{3}y\left(\frac{\partial U}{\partial t} + U\frac{\partial U}{\partial x}\right)\right\} . \tag{2.43}$$

Near the point $\tau_w = 0$, τ_w can be expanded in the form

$$\tau_w = \frac{\partial \tau_w}{\partial x}(x - x_s) + \frac{\partial \tau_w}{\partial t}(t - t_s) + \dots . \tag{2.44}$$

At the time $t = t_s$, the stream function ψ becomes

$$\psi = \frac{y^2}{2\rho\nu}\left\{\frac{\partial \tau_w}{\partial x}(x - x_s) - \frac{\rho}{3}y\left(\frac{\partial U}{\partial t} + U\frac{\partial U}{\partial t}\right)\right\} . \tag{2.45}$$

The quantity in brackets shows that a dividing streamline starts at the point $x = x_s$ ($\tau_w = 0$), and its inclination, $\tan \alpha$, is expressed as

$$\tan \alpha = \frac{\frac{\partial \tau_w}{\partial x}}{\frac{\rho}{3}\left(\frac{\partial U}{\partial t} + U \frac{\partial U}{\partial x}\right)} \quad . \tag{2.46}$$

A positive value of $\tan \alpha$ means that the flow is upwards, *i.e.*, there is a separation. A negative value corresponds to a reattachment, and zero value corresponds to simple turning of τ_w .

For the separation in one swing period ($U > 0$) of oscillatory motion, we can safely assume that

$$\frac{\partial \tau_w}{\partial x} < 0 \quad , \tag{2.47}$$

$$\frac{\partial U}{\partial t} + U \frac{\partial U}{\partial x} < 0 \quad . \tag{2.48}$$

Eq. (2.48) is almost satisfied by the $\overline{U}'$ value of Eq. (2.38). Substituting Eq. (2.37) into Eq. (2.47), we can obtain an additional condition for separation in oscillatory flow in the following simple form:

$$\frac{d^2 \overline{U}}{dx^2} < 0 \quad . \tag{2.49}$$

On the contrary, $\overline{U}'' > 0$ shows an attachment. Eqs. (2.41) and (2.49) can be used to obtain the location of the separation point at a given instant.

From the present analysis of Schlichting's solution for an oscillatory boundary layer, it can be concluded that the separation point is determined by the derivative of the edge velocity along the surface, *i.e.*, the pressure gradient. Before the end of one swing, the separation point moves upstream across the point of zero pressure gradient. These features are the same as those obtained in the preceding section.

When we use potential flow theory to obtain the edge velocity distribution along the surface, we can roughly predict the location of the separation point by applying the criterion formula in this section. However, more precise treatment of the outer and inner flows would be necessary to obtain an accurate prediction of the separation and the attachment points. The present analysis is a starting step for the problem of flow separation from a smooth surface.

3. SHARP-EDGE SEPARATION

The problem of the separation at a sharp-edge corner is also important for estimating hydrodynamic forces on an oscillating bluff body like a ship. In this chapter, an attempt is made to obtain the forces in a quite simple way. Instead of expressing the separated flow in terms of vortex sheets shed from the edges, an assumption is made that one or two concentrated vortices can be used. In the following two sections, the motions of a flat plate normal to its plane are discussed.

3.1 Starting Motion of a Flat Plate

To obtain the normal force on a flat plate starting from rest with a constant velocity, the following simple procedures are adopted:

i) Put a pair of vortices at the midpoints of the path lines of the separating edges (see Fig. 3.1).

ii) Determine the vortex strength by Kutta condition.

To begin, suppose that the flat plate of breadth 2 in the z plane is mapped into a segment of length 2 in the ζ plane, as shown in Fig. 3.1. The edge $z = i$ corresponds to $\zeta = 0$. The mapping function is

$$z = \sqrt{\zeta^2 - 1} \ . \tag{3.1}$$

Then assume that a vortex of strength Γ lies on each of the path lines of the separating edges at an arbitrary distance x_0 from the edge:

$$z = z_0 = x_0 + i \ ,$$

or

$$\zeta = \zeta_0 = \xi_0 + i\eta_0 \tag{3.2}$$

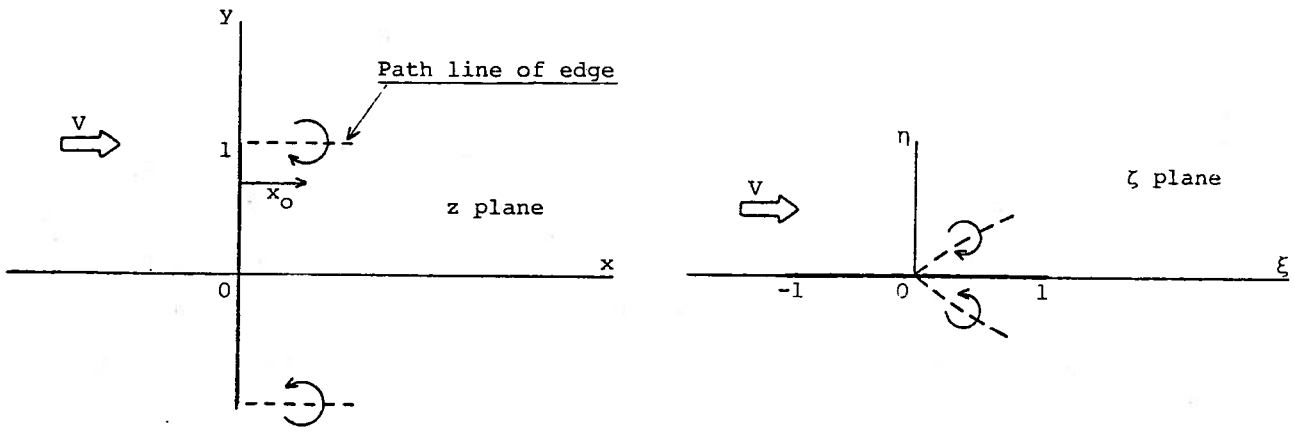

Figure 3.1. Assumed pair of vorticies behind a flat plate starting from rest

in the ζ plane. The two vortices have opposite directions of rotation.

If the flow is described with reference to the plate, there is an incident stream of velocity $V(t)$, as shown in Fig. 3.1. The fluid velocity can be expressed in terms of the [complex] conjugate velocity, that is,

$$\bar{q}(z) = u(x,y) - iv(x,y) = \bar{Q}(\zeta)/\frac{dz}{d\zeta} , \tag{3.3}$$

where

$$\bar{Q}(\zeta) = V + \frac{1}{2\pi i}\left(\frac{\Gamma}{\zeta - \zeta_0} - \frac{\Gamma}{\zeta - \bar{\zeta}_0}\right) . \tag{3.4}$$

At the edge point $z = i$ or $\zeta = 0$, the Kutta condition is applied to determine the vortex strength Γ :

$$\Gamma = - 2\pi V\left(\frac{i\,\zeta_0\bar{\zeta}_0}{\zeta_0 - \bar{\zeta}_0}\right) \tag{3.5}$$

$$= - 2\pi V\frac{\sqrt{x_0}}{2\sqrt{2}}\sqrt{x_0^2 + 4}\,\left[x_0 + \sqrt{x_0^2 + 4}\right]^{1/2} . \tag{3.6}$$

For small values of x_0, this becomes approximately

$$\Gamma \simeq - 2\pi V\sqrt{x_0} . \tag{3.7}$$

The vortex is assumed to lie on the midpoint of the path length s of the edge:

$$x_0 = \frac{s}{2} = \frac{1}{2}V t . \tag{3.8}$$

The force on the plate is easily derived from the impulsive momentum I of the flow field,

$$F = \frac{dI}{dt} = \frac{d}{dt}\{\rho\pi b^2 V - 2\rho y_0 \Gamma\} , \tag{3.9}$$

where b = half-breadth = 1 , $y_0 \equiv 1$. Then

$$F = \pi\rho\frac{dV}{dt} - 2\rho\frac{d\Gamma}{dt} . \tag{3.10}$$

From Eqs. (3.7) and (3.8), the first approximation of Γ for small x_0 is

$$\Gamma \simeq -2\pi V\sqrt{Vt/2} . \tag{3.11}$$

The force can be calculated in the form

$$C_N = \frac{F}{(1/2)\rho\cdot 2bV^2} = \sqrt{2}\pi/\sqrt{t'} , \tag{3.12}$$

with $t' = Vt$. Figs. 3.2 and 3.3 show results calculated from Eqs. (3.11) and (3.12). Eq. (3.11) becomes quite close to Wedemeyer's exact solution [3]. Eq. (3.12) is also acceptable compared to Kudo's calculation [4].

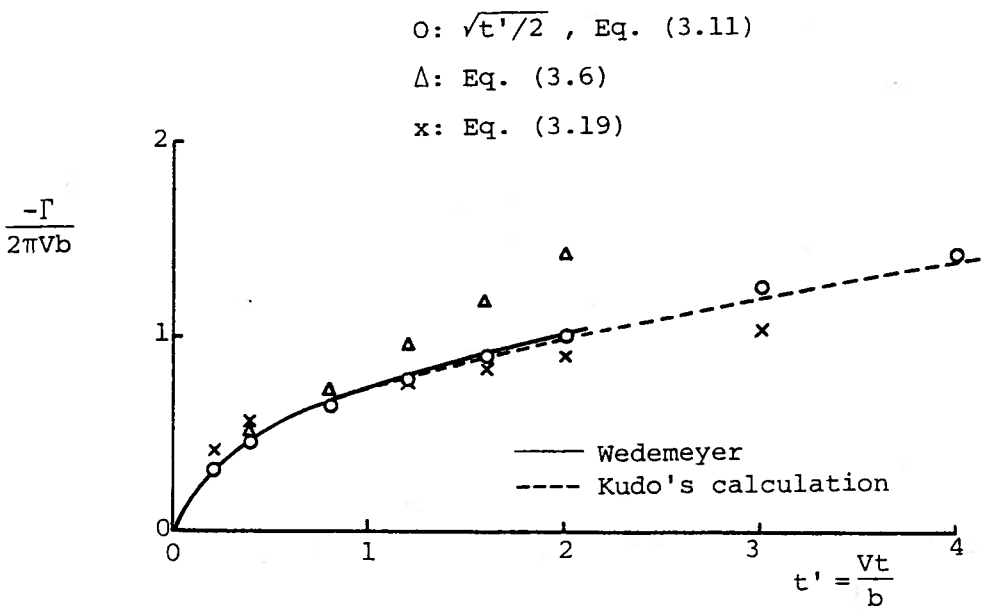

Figure 3-2. Vortex generation in starting motion of flat plate of half-breadth b=1.

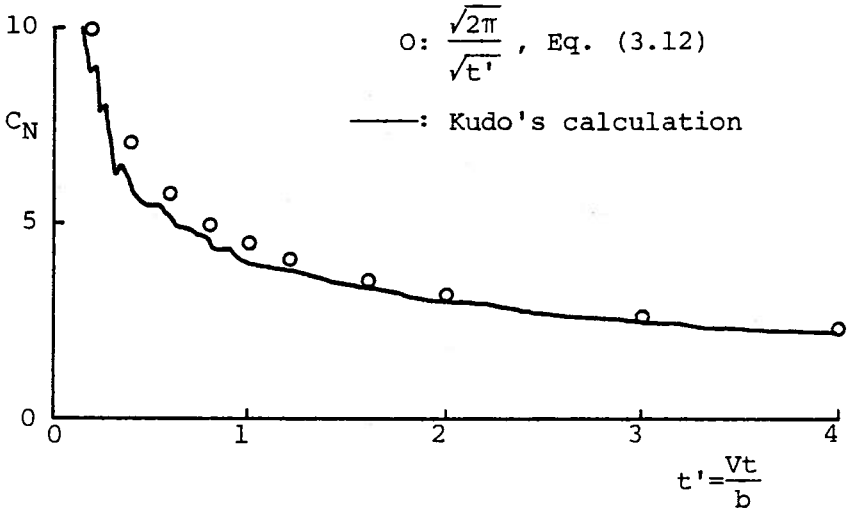

Figure 3-3. Normal force on flat plate in starting motion

The success of this simple approach can be understood in the following way: The velocity $\bar{q}_v$ at a vortex position can be obtained by dropping the term corresponding to that vortex. Thus,

$$\bar{q}_v = \bar{Q}_v / \frac{dz}{d\zeta} \tag{3.13}$$

and

$$\bar{Q}_v = V\left(1 + \frac{\zeta_0 \bar{\zeta}_0}{(\zeta_0 - \bar{\zeta}_0)^2}\right) = V\left(1 - \frac{x_0\sqrt{x_0^2+4}}{2(x_0\sqrt{x_0^2+4} - x_0^2)}\right) . \tag{3.14}$$

So we find that

$$\bar{Q}_v \simeq \frac{V}{2} \quad \text{as} \quad x_0 \to 0 . \tag{3.15}$$

Eq. (3.15) means that the vortex velocity is half of the velocity in the absence of that vortex pair. Although this does not mean that the location of the vortex is on the half-way point of the path of the edge, this fact is quite interesting.

If we again assume that the vortex lies on the line $y_0 \equiv 1$ and obtain the distance x_0 from the edge by solving the equation

$$\frac{dx_0}{dt} = u_V(x_0) = Re\{\bar{q}_V\}$$

$$= V/4\sqrt{x_0} \quad \text{for small } x_0 , \tag{3.16}$$

the result is

$$x_0 = \left(\frac{3}{8}\int_0^t V dt\right)^{2/3} . \tag{3.17}$$

Applying this to the case of starting motion,

$$x_0 = \left(\frac{3}{8} V t\right)^{2/3} , \tag{3.18}$$

and substituting this into Eq. (3.7), we obtain

$$\Gamma = - 2\pi V\left(\frac{3}{8} V t\right)^{1/3} . \tag{3.19}$$

Eq. (3.19) is also shown in Fig. 3.2 and gives slightly lower values than Eq. (3.11) in the range $Vt > 1$.

On the other hand, Eq. (3.6), the original expression, gives higher values when x_0 is taken as $s/2$, the midpoint. Therefore we can realize that Eq. (3.11) compensates two errors, one arising from the assumption of vortex location ($x_0 = s/2$), and the other coming from the simplification of the Γ expression.

There seems to be no evidence for the present assumption, Eq. (3.8), on the vortex location. However, we can cite here some support, for instance, Pierce's photograph [5], Bollay's assumption that the trailing vortex of a low-aspect-ratio wing sheds at half the angle of incidence, and the numerical calculations made by Fink and Soh [3] and Kudo [4].

In conclusion, it can be said that the present simple approach predicts the force on a flat plate with good accuracy. However, it can not be expected that this method will also give a valid detailed description of the flow field.

3.2 Oscillatory Motion of a Flat Plate

According to the observations by Ikeda *et al* [2] and the numerical calculations by Kudo [4] and by Fink and Soh [5], the flow around a flat plate oscillating normal to its plane is quite interesting.

Roughly speaking, a pair of vortex-sheet cores is created during each swing of the body. However, toward the end of a swing, before the plate motion ceases, the sign of the vorticity density near the edge becomes opposite to that of the vortex core created during the swing. This means that the strength of the shed vorticity has a phase lead with respect to the velocity of the plate. The physical interpretation of this fact seems to be that the velocity at the rear side of the edge induced by the vortex core just created becomes greater than the velocity on the front side near the edge.

During the next swing, the previous vortex moves downstream past the plate and a new vortex core is generated behind the plate. According to the calculations by Kudo or by Fink and Soh, the location of the previous vortex is nearly above the newly-created vortex. During continuous oscillatory sway motion, the vortices thus created seem to flow away from the plate.

In order to formulate this kind of flow mathematically, we can again apply the idea in the preceding section. With the coordinates fixed on the body, the upstream velocity can be expressed

$$V = \overline{V} \sin \omega t \quad , \quad \overline{V} = \omega X \quad . \tag{3.20}$$

Assume that the flow field is represented by two pairs of concentrated vortices which lie somewhere on the horizontal lines through the edges. Suppose their distances from the edge are x_0 and x_1 and their strengths Γ_0 and Γ_1, as shown in Fig. 3.4. When the flow goes right ($V > 0$), we assume that Γ_0 represents the pre-

vious vortex, which is constant, and Γ_1 the new one, which is growing with time.

Assume that the total circulation in the upper half plane is of the form

$$\Gamma = \bar{\Gamma} \cos(\omega t + \varepsilon) , \quad (3.21)$$

with the amplitude $\bar{\Gamma}$ and the phase lead ε. At the time $\omega t = -\varepsilon$, there is only a pair of vortices, the strength of which is

$$\Gamma_0 = \bar{\Gamma} . \quad (3.22)$$

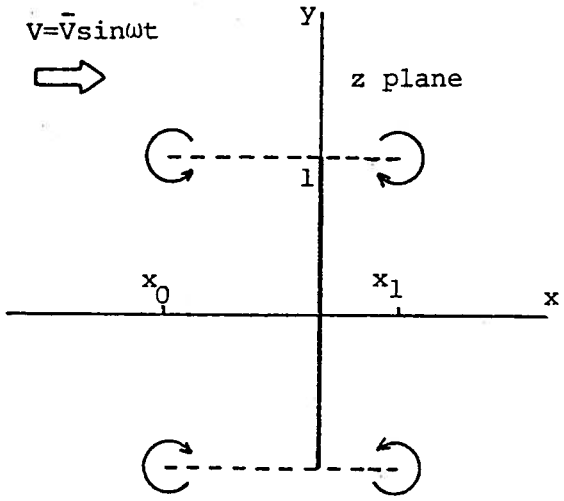

Figure 3.4. Two-vortex-pair model for oscillating flat plate

Thereafter Γ_0 is constant. However, a new pair, of strength Γ_1, grows with time until it reaches its maximum value,

$$\Gamma_1 = -2\bar{\Gamma} \quad \text{at} \quad \omega t = \pi - \varepsilon . \quad (3.23)$$

At $\omega t = \pi - \varepsilon$, the total circulation Γ equals $-\bar{\Gamma}$, that is,

$$\Gamma = \Gamma_0 + \Gamma_1 = -\bar{\Gamma} \quad \text{at} \quad \omega t = \pi - \varepsilon . \quad (3.24)$$

However, the flow field should again be expressed by one pair of vortices of strength Γ_1 at $\omega t = \pi - \varepsilon$, so that the previous vortex should be mixed into the new vortex Γ_1 at $\omega t = \pi - \varepsilon$. In other words, Γ_0 has traveled along an unknown route and joined with the new vortex Γ_1 at $\omega t = \pi - \varepsilon$. In this model, we do not concern ourselves with the path of the vortex Γ_0. Instead, we have assumed the variation of Γ as in Eq. (3.21).

To determine the vortex strengths, we apply the Kutta condition at the edges of the plate. At $\omega t = -\varepsilon$, there is a vortex pair

Γ_0 . The velocity at the edge $z = i$ or $\zeta = 0$ can be expressed in the ζ plane by using the same mapping function as in Eq. (3.1):

$$\overline{Q} = V + \frac{\Gamma_0}{2\pi i}\left(\frac{1}{\zeta - \zeta_0} - \frac{1}{\zeta - \overline{\zeta}_0}\right)\Bigg|_{\substack{\omega t = -\varepsilon \\ \zeta = 0}} . \tag{3.25}$$

The Kutta condition($\overline{Q} = 0$) requires that

$$\Gamma_0 = - 2\pi i V \frac{\zeta_0 \overline{\zeta}_0}{\zeta_0 - \overline{\zeta}_0} . \tag{3.26}$$

For small values of x_0 , this becomes

$$\Gamma_0 = 2\pi\sqrt{|x_0|}\,\overline{V}\sin\varepsilon = \overline{\Gamma} . \tag{3.27}$$

At times such that $\omega t > -\varepsilon$, there are two vortex pairs, Γ_0 and Γ_1 . The Kutta condition for the growing vortex Γ_1 can be written in the form

$$\overline{Q} = V(t) + V_0(t) + \frac{\Gamma_1}{2\pi i}\left(\frac{1}{-\zeta_1} - \frac{1}{-\overline{\zeta}_1}\right) = 0 , \tag{3.28}$$

or

$$\Gamma_1 = - 2\pi\sqrt{x_1}\,[V + V_0] \qquad \text{for small } x_1 , \tag{3.29}$$

where V_0 represents the induced velocity of the previous vortex, the strength of which (Γ_0) is now constant. But the location of Γ_0 is now unknown, so that V_0 is unknown.

For the growing vortex Γ_1 , we assume the velocity $\dot{x}_1$ as follows:

$$\dot{x}_1 = \frac{1}{2}[V + V_0] \quad \text{for} \quad -\varepsilon < \omega t < \pi - \varepsilon . \tag{3.30}$$

The quantity $V + V_0$ is the velocity at $\zeta = 0$ in the ζ plane, which means that the incoming velocity at the edge has increased by the amount V_0 due to the effect of the previous vortex. This assumption is similar to the one that the vortex lies on the mid-point of the travel path of the edge.

From Eqs. (3.28), (3.29), and

$$\Gamma_1 = \Gamma - \Gamma_0 = \overline{\Gamma}\{\cos(\omega t + \varepsilon) - 1\} , \tag{3.31}$$

we can obtain x_1 :

$$\frac{8}{3}\pi x_1^{3/2} = \frac{\overline{\Gamma}}{\omega}\{\omega t + \varepsilon - \sin(\omega t + \varepsilon)\} \quad . \tag{3.32}$$

It should be noted that we have not assumed the form of V_0 . At the instant $\omega t = \pi - \varepsilon$, Eq. (3.32) becomes

$$\frac{8}{3} x_1^{3/2} = \frac{\overline{\Gamma}}{\omega} \quad , \tag{3.33}$$

and, from symmetry of the vortex locations between the times $\omega t = -\varepsilon$ and $\pi - \varepsilon$, we obtain another relation from Eq. (3.27):

$$x_1 = |x_0| = \left(\frac{\overline{\Gamma}}{2\pi\overline{V}\sin\varepsilon}\right)^2 \quad . \tag{3.34}$$

Eqs. (3.33) and (3.34) can be arranged into the forms:

$$\overline{\Gamma} = \left(2\pi\sin\varepsilon\right)^{3/2}\left(\frac{3}{8}\right)^{1/2} X\,\omega\sqrt{X} \quad ; \tag{3.35}$$

$$x_1 = \frac{3\pi}{4}(\sin\varepsilon)\,X \quad . \tag{3.36}$$

Note that x_1 or x_0 is now the vortex location at the time when its strength becomes maximum, that is, at $\omega t = \varepsilon$ or $\pi - \varepsilon$.

Assumption on the phase. The phase lead ε of the circulation Γ with respect to the velocity V plays an important role in this analysis. It is introduced to express an effect of the previous swing. However, it is still not clear what is a reasonable condition to determine the value of ε . Here we assume the value to be

$$\varepsilon = \frac{\pi}{4} = 45° \quad . \tag{3.37}$$

The support of this assumption can be found in several examples of viscous flow theory. For instance, the shear stress in the oscillatory boundary layer has the same phase. Kudo's numerical calculation also showed a phase lead of about $\pi/4$ in the case of flat-plate sway. We can expect that the phase lead $\pi/4$ might be derived from a high-frequency expansion of the equation system for this kind of flow. The problem is left for future study.

The force can be obtained by taking the time derivative of the impulsive momentum of the flow field:

$$F = \rho \pi \frac{dV}{dt} - 2 \rho \frac{d\Gamma}{dt} \quad . \tag{3.38}$$

Thus,

$$F = \rho \{ \pi X \omega^2 + 2 \beta X \omega^2 \sqrt{X} \sin \varepsilon \} \cos \omega t + 2 \rho \beta X \omega^2 \sqrt{X} \cos \varepsilon \sin \omega t \quad , \tag{3.39}$$

where

$$\beta = \left(2 \pi \sin \varepsilon \right)^{3/2} \left(\frac{3}{8} \right)^{1/2} = 5.735 \quad \text{for} \quad \varepsilon = \pi/4 \quad . \tag{3.40}$$

In this analysis, the force has only simple-harmonic components at the fundamental frequency of oscillation. In order to compare the result with other results, we have to transform the damping term into the usual nonlinear form:

$$F = C_m \rho \pi X \omega^2 \cos \omega t + C_D \cdot \frac{\rho}{2} \cdot 2 \cdot X^2 \omega^2 \sin^2 \omega t \quad . \tag{3.41}$$

Equating the work done in one swing period, as derived from Eqs. (3.39) and (3.41), we obtain

$$C_D = \frac{3}{4} \pi \beta \cos \varepsilon \cdot \frac{1}{\sqrt{X}} = \frac{9.555}{\sqrt{X}} \quad \text{for} \quad \varepsilon = \pi/4 \quad , \tag{3.42}$$

$$C_m = 1 + \frac{2}{\pi} \beta \sin \varepsilon \sqrt{X} = 1 + 2.582 \sqrt{X} \quad \text{for} \quad \varepsilon = \pi/4 \quad . \tag{3.43}$$

Figures 3.5 and 3.6 show the comparison of Eqs. (3.42) and (3.43) with the numerical calculations by Kudo, and the Keulegan and Carpenter experiments. The agreement of the C_D values is quite good, while C_m agrees with Kudo's calculation, which is about twice as large as the value from the Keulegan and Carpenter experiments. The reason for this discrepancy is still unknown.

The conclusion of this section can be summarized as follows: A simple approach to the problem of a flat plate oscillating normal to its plane is attempted. The flow field is represented by two pairs of vortices. The variation of the vortex strength is assumed

to be sinusoidal and the vortex velocity to be half the flow velocity at the separating edge. An additional assumption on the phase lead of the vortex strength is also made. With the Kutta condition satisfied at the edge, the results are expressed in simple forms and agree with other works, especially for C_D .

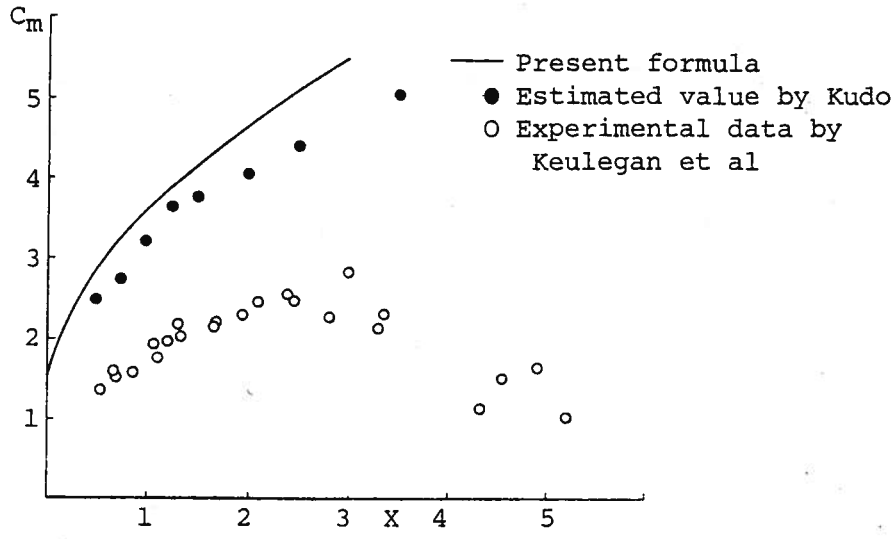

Figure 3.5. Added-mass coefficient of oscillating flat plate

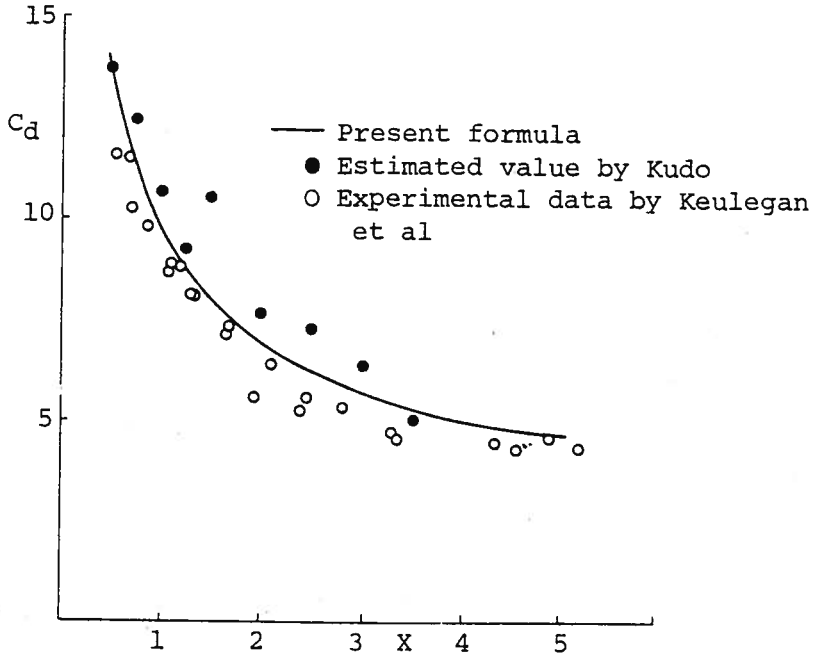

Figure 3.6. Drag coefficient of oscillating flat plate

4. VORTEX-SHEET FORMATION AROUND SHIP HULL

This chapter describes an outline of an idea and a procedure for the numerical computation of vortex formation around an oscillating ship hull with and without forward speed. The method is based on the slender-body assumption which enables us to treat the problem in the two-dimensional plane of the cross-sections.

However, a difficulty has arisen in the numerical computation, not because of a defect of the basic concept but mainly because of the difficulty of treatment of the self-crossing of the vortex sheet in an oscillatory motion. This situation is also described.

Although the numerical results have not been obtained, it is worthwhile to state the procedure briefly.

4.1 Basic Assumption and Procedure

The objective is to obtain the flow field around a ship, as well as the force and moment when the ship is moving forward and oscillating in, say, roll. Neglecting wave effects and skin friction, we reduce the problem to that of predicting the separating flow around the hull. This can be represented by a vortex-sheet system shedding from separation points on the hull if we neglect the viscous diffusion of vorticity. Recent calculations on the vortex-sheet configuration in unsteady two-dimensional flow, carried out by Fink and Soh [3] and Kudo [4], showed us that this kind of treatment can predict the forces on the body fairly well. Thus we can expect that this approach could be applied to a ship hull form providing that the separation-point condition is treated in an appropriate way.

The following three basic assumptions are made in the present method:

i) Only longitudinal vortices are shed at the shedding points in the cross-sectional plane (see the coordinate system in Fig. 4.1). According to Fuwa's [6] analysis, which is based on the slender-body assumption, the problem can be treated in the two-dimensional plane of each section. In this case, the longitudinal component ω_x of the vorticity is dominant, so that ω_y , $\omega_z = o(\omega_x)$ and y , $z = o(x)$.

ii) The shed vortex is convected downstream with the forward velocity U without change of strength. This assumption might seem to be rough compared to that of the slender-body theory. It should be considered as a first step for the vortex convection in the longitudinal direction.

iii) The separation point is treated in two ways, as a sharp-edge separation and as a smooth-surface separation. The former can be treated in the same way as in the recent works [3][4]. For the latter, the position of the separation point can be predicted by boundary-layer theory, with the potential-flow velocity field as described in a previous chapter of this paper.

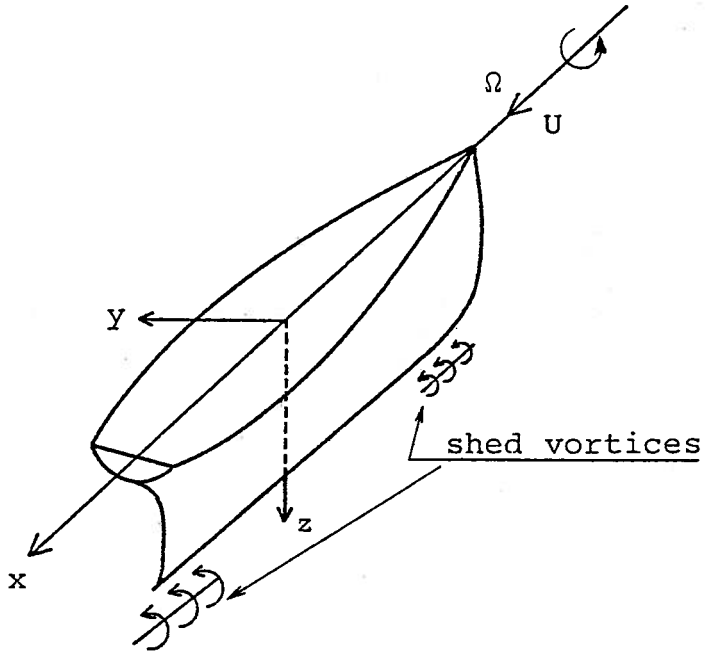

Figure 4.1. Coordinate System

The general procedure is to carry out a time integration of the vortex-path equation by using the velocity field at the instant, and to find the location and the strength of a newly shed vortex at each time step. To begin with, the following three pre-calculations are needed:

i) Representation of the hull form by a mapping function transforming the section shape into a circle.

ii) Calculation of the potential-flow field around the hull in the presence of ship forward speed and roll velocity, using slender-body theory.

iii) Calculation of the separation point in each cross-section as a function of time t in one roll swing, using the girthwise distribution of crossflow velocity amplitude and its derivatives. When the value of the first derivative is large enough, the point is taken as a sharp edge.

The time-step integration is carried out in the following way:

iv) Calculation at the shedding point to determine the velocity, the direction, and the strength of the newly-shed vortex sheet.

v) Calculation of the vortex-sheet velocity.

vi) Calculation of the moment acting on the ship.

vii) Time integration to obtain the new position and strength of the vortex sheet at the time after one time step. The procedure from iv) to vii) is repeated for several swing periods of the motion.

4.2 Formulation

With the coordinates as in Fig. 4.1, the ship section shape can be represented by a Lewis form:

$$\chi = y + iz$$
$$= a_1\zeta + a_2\zeta^{-1} + a_3\zeta^{-3} \ . \qquad (4.1)$$

The velocity potential $\Phi(x,y,z,t)$ is expressed in the form

$$\Phi = Ux + Re\{UF_1 + \Omega F_2 + F_3\} \ , \qquad (4.2)$$

where U and Ω are the ship forward velocity and the roll angular velocity, respectively. The complex potential F_1 at each section corresponds to the forward motion and is obtained from Tuck and von Kerczek's expression [7]. The potential F_2 due to the ship roll motion is also obtained by assuming that the double body of the section rotates around the point O. This can be written

$$F_2 = -i\{a_2(a_1 + a_3)\zeta^{-2} + a_1a_3\zeta^{-4}\} \ . \qquad (4.3)$$

The potential F_3 represents the vortex-sheet potential which is expressed in the form

$$F_3 = \frac{1}{2\pi i}\int_{s_1}^{s_2} \log\left(\frac{\zeta - \zeta_1}{\zeta - 1/\bar{\zeta}_1}\cdot\frac{\zeta + \zeta_1}{\zeta + 1/\bar{\zeta}_1}\right)\gamma(\zeta_1)\ ds \ , \qquad (4.4)$$

where ζ_1 lies on the vortex sheet where the vorticity density is γ, and ds is the length element of the sheet. The integration should cover all sets of vortex sheets in the double-body section.

The shedding condition can be given in the following ways: When separation occurs on the smooth surface, the location of the separation point can be derived from the boundary-layer theory, *i.e.*, from Eq. (2.41), at a prescribed time t during the swing. The vortex sheet is assumed to shed tangentially to the surface, so that the density γ and the velocity q_{vs} of the vortex sheet can be given as

$$\gamma = |q_{rt}| \ , \quad q_{vs} = \frac{1}{2}\, q_{rt} \ , \qquad (4.5)$$

where q_{rt} represents the relative tangential velocity at the

separation point, which can be obtained approximately from the potential F_2 . When the separating edge is sharp, the shedding condition is given in a manner similar to that of Fink and Soh's treatment, in which the density is determined by a Kutta condition at the edge and the velocity is calculated at a point a small distance away from the edge.

Since it is not easy to transform an arbitrary point in the real plane into the mapped ζ plane, we carry out all of these calculations in the ζ plane, noting that in the transformation the strength of the circulation, $\gamma\, ds$, remains constant, so that the density changes by the rate of $|d\chi/d\zeta|$.

In the numerical calculation, the vortex sheet is discretized by a finite number of vortex-sheet segments of small length, with linear variation of vorticity density on each segment. The time integration is carried out by Euler's scheme.

4.3 Discussion

According to the procedure briefly mentioned above, the numerical calculation was carried out for the case of a flat plate ($L \times B \times 2d = 2 \times 0 \times 0.4$) starting to roll around its central axis without forward velocity. Fig. 4.2 shows an example of the result of the vortex-sheet generation relative to the body axis. As time proceeds, a vortex sheet is created on the right-hand side of the plate during the first swing and then it flows to the other side in the second swing. At a particular moment, the vortex sheet crosses itself, and the calculated moment shows scattering, as in Fig. 4.2. Since this kind of vortex-sheet crossing is not expected in the real flow, there must be a defect in the numerical procedure. Several attempts have been made concerning the time-step interval, the shedding-point condition, *etc*. However, the difficulty could not be removed.

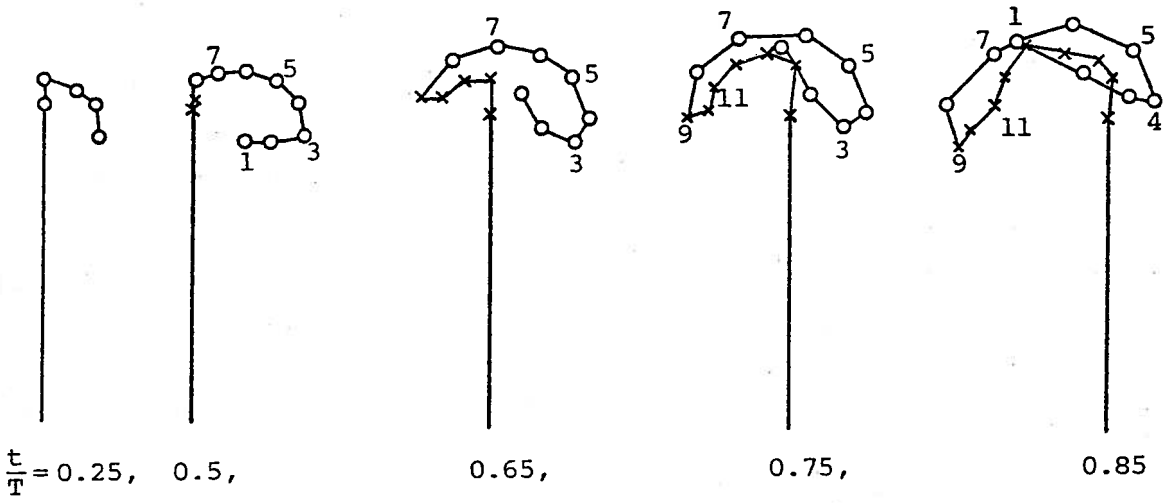

$\frac{t}{T}$ = 0.25, 0.5, 0.65, 0.75, 0.85

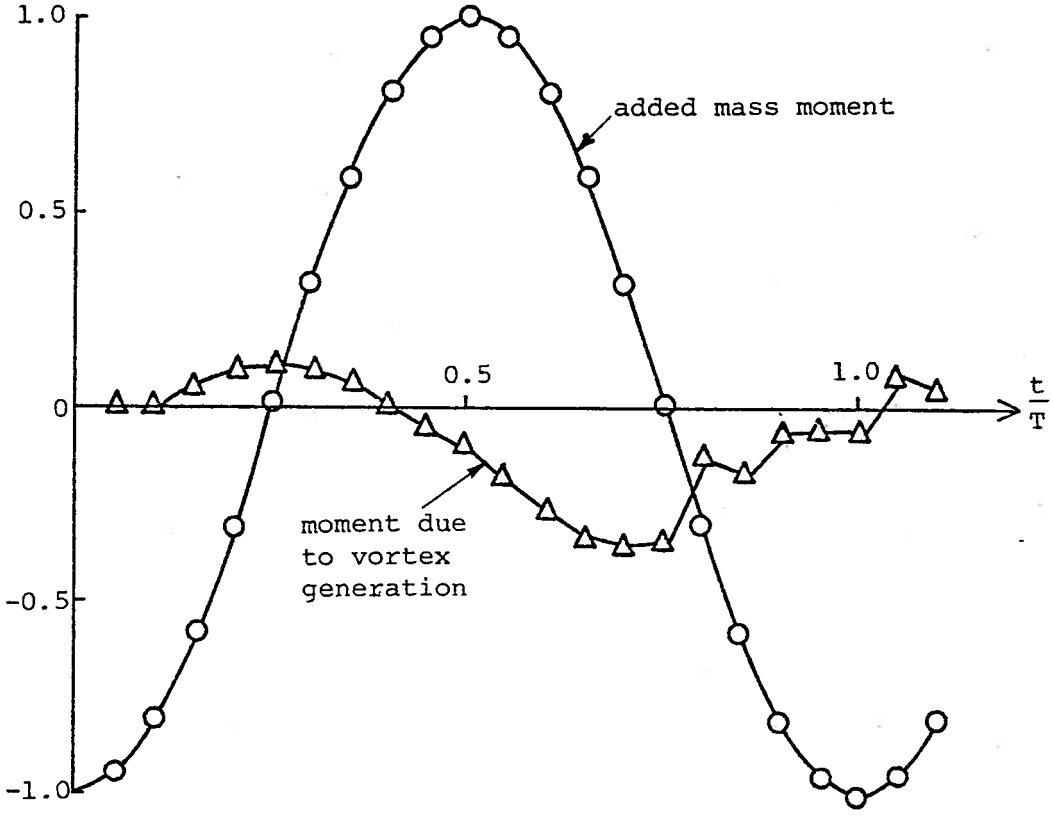

Figure 4.2. Vortex-sheet formation and moment variation of rolling flat plate with amplitude 10°.

The same phenomenon appeared in the calculations by Kudo [4] and Fink and Soh [3], who discretized the vortex sheet into a number of concentrated point vortices. In those treatments, the vortex-sheet crossing might not greatly affect the calculation of the force or the time integration of the sheet configuration. In the present case, however, the crossing becomes a definite difficulty so that further time steps cannot be achieved.

Although the present trial calculation has not been successful, the basic idea of the present method still seems to be worth pursuing. The performance of this calculation must be left for a future study.

5. CONCLUSION

Three different approaches have been made to the problem of flow separation in unsteady motion of a body. In Chapter 2, separation from a smooth curved surface is discussed from the view of boundary-layer theory. It is found through the analyses of a starting motion and of an oscillatory motion that the separation point depends mainly on the amplitude ratio, providing that the ratio is small.

The problem of the sharp-edge separation is discussed in a quite simple way through the use of a small number of vortex pairs. This method is applied to the starting and oscillatory motions of a flat plate, the motion being normal to the plane of the plate. The force is expressed in a simple formula, which agrees well with experiments and with others' numerical computations.

In the last chapter, a procedure to obtain the vortex-sheet formation around a ship hull oscillating and moving forward is described. Although the numerical calculation has not been completed, because of the difficulty of the numerical treatment of a two-dimensional vortex-sheet configuration, the procedure itself seems to be adequate. A slight improvement of the vortex calculation might make the method work well.

The author believes that these discussions and analyses constitute a useful step toward the final goal of the prediction of ship viscous roll damping.

ACKNOWLEDGMENT

This work has been done during the author's stay at The University of Michigan for a year. The author would like to express his heartfelt appreciation to Professor T. Francis Ogilvie, Professor William S. Vorus, and Mr. John P. Hackett for their valuable advice, discussions, and continuous encouragement.

The author also feels grateful to Professor Norio Tanaka and Dr. Yoshiko Ikeda of the University of Osaka Prefecture.

REFERENCES

1. Schlichting, H., *Boundary Layer Theory*, 6th Ed. McGraw-Hill (1968)

2. Ikeda, Y., and Fukutomi, "The Drag on Oscillating Flat Plate and Circular Cylinder at Low K-C Number," unpublished (1979).

3. Fink, P. T., and Soh, W. K., "Calculation of Vortex Sheets in Unsteady Flow and Applications in Ship Hydrodynamics," *10th Symp. on Naval Hydrodynamics* (1974)

4. Kudo, K., "An Inviscid Model of Discrete-Vortex Shedding for Two-Dimensional Oscillating Flow Around a Flat Plate," *Jour. Soc. Naval Arch. of Japan*, Vol. 145 (1979)

5. Pierce, D., "Photographic Evidence of the Formation and Growth of Vorticity Behind Plates Accelerated from Rest in Still Water," *Jour. Fluid Mech.*, Vol. 11 (1961)

6. Fuwa, T., "Hydrodynamic Forces Acting on a Ship in Oblique Towing," *Jour. Soc. Naval Arch. of Japan*, Vol. 134 (1973)

7. Tuck, E. O., and Von Kerczek, C., "Streamlines and Pressure Distribution on Arbitrary Ship Hulls at Zero Froude Number," *Jour. Ship Research*, Vol. 12 (1968)

DISTRIBUTION LIST FOR REPORTS PREPARED UNDER THE
GENERAL HYDROMECHANICS RESEARCH PROGRAM

25 Commander
David W. Taylor Naval Ship
R&D Center (Attn: Code 1505)
Bethesda, MD 20084

1 Officer-in-Charge
Annapolis Laboratory
David W. Taylor Naval
Ship R&D Center (Code 522.3)
Annapolis, MD 21402

9 Commander
Naval Sea Systems Command
Washington, DC 20362
Attn: SEA 32R
312
3213
05H
05R11
52
521
524
99612

12 Director
Defence Documentation Center
5010 Duke Street
Alexandria, VA 22314

1 Office of Naval Research
800 N. Quincy Street
Arlington, VA 22217
Attn: Mr. R.D. Cooper (Code 438)

1 Office of Naval Research
Branch Office (493)
536 S. Clark Street
Chicago, IL 60605

1 Chief Scientist
Office of Naval Research
Branch Office
1030 E. Green Street
Pasadena, CA 91106

1 Office of Naval Research
Resident Representative
715 Broadway (5th Floor)
New York, NY 10003

1 Office of Naval Research
San Francisco Area Office
760 Market Street, Room 447
San Francisco, CA 94102

1 Director (Code 2027)
Naval Research Laboratory
Washington, DC 20390

1 Commander
Naval Facilities Engineering
Command (Code 032C)
Washington, DC 20390

1 Library of Congress
Science & Technology Division
Washington, DC 20540

1 Naval Ship Engineering Center
Norfolk Division
Combatant Craft Engr Dept
Attn: D. Blount (6660)
Norfolk, VA 23511

1 Commander (ADL)
Naval Air Development Center
Warminster, PA 18974

1 Naval Underwater Weapons Research
& Engineering Station (Library)
Newport, RI 02840

1 Commanding Officer (L31)
Naval Civil Engineering Laboratory
Port Hueneme, CA 93043

1 Hydronautics, Inc. (Library)
Pindell School Rd
Laurel, MD 20810

1 McDonnel Douglas Aircraft Co.
3855 Lakewood Blvd
Long Beach, CA 90801
Attn: Dr. T. Cebeci

1 Newport News Shipbuilding and
Dry Dock Company (Tech Library)
4101 Washington Avenue
Newport News, VA 23607

1 Mr. S. Spangler
Nielsen Engineering & Research, Inc.
510 Clyde Avenue
Mountain View, CA 94043

1 Society of Naval Architects and
Marine Engineers (Tech Library)
One World Trade Center, Suite 1369
New York, NY 10048

1 Sun Shipbuilding & Dry Dock Co.
Attn: Chief Naval Architect
Chester, PA 19000

1 Sperry Systems Management Division
Sperry Rand Corporation (Library)
Great Neck, NY 11020

1 Stanford Research Institute
Attn: Library
Menlo Park, CA 94025

2 Southwest Research Institute
P.O. Drawer 28510
San Antonio, TX 78284
Attn: Applied Mechanics Review
Dr. H. Abramson

1 Tracor, Inc.
6500 Tracor Lane
Austin, TX 78721

1 Mr. Robert Taggart
9411 Lee Hgwy, Suite P
Fairfax, VA 22031

1 Ocean Engr Department
Woods Hole Oceanographic Inc.
Woods Hole, MA 02543

1 Worcester Polytechnic Inst.
Alden Research Lab (Tech Library)
Worcester, MA 01609

1 Applied Physics Laboratory
University of Washington (Tech Library)
1013 N.E. 40th Street
Seattle, WA 98105

4 University of California
Naval Architecture Department
Berkeley, CA 94720
Attn: Prof. W. Webster
Prof. J. Paulling
Prof. J. Wehausen
Library

3 California Institute of Technology
Pasadena, CA 91109
Attn: Dr. T.Y. Wu
Dr. A.J. Acosta
Library

1 Docs/Repts/Trans Section
Scripps Institute of Oceanography
Library
University of California, San Diego
P.O. Box 2367
La Jolla, CA 92037

1 Engineering Research Center
Reading Room
Colorado State University
Foothills Campus
Fort Collins, CO 80521

2 Florida Atlantic University
Ocean Engineering Department
Boca Raton, FL 33432
Attn: Technical Library
Dr. S. Dunne

4 Commander
Naval Ocean Systems Center
San Diego, CA 92152
Attn: Dr. A. Fabula (4007)
Dr. J. Hoyt (2501)
Dr. M. Reichman (6342)
Library

1 Library
Naval Underwater Systems Center
Newport, RI 02840

1 Research Center Library
Waterways Experiment Station
Corp of Engineers
P.O. Box 631
Vicksburg, MS 39180

1 Charleston Naval Shipyard
Technical Library
Naval Base
Charleston, SC 29408

1 Norfolk Naval Shipyard
Technical Library
Portsmouth, VA 23709

1 Portsmouth Naval Shipyard
Technical Library
Portsmouth, NH 03801

1 Puget Sound Naval Shipyard
Engineering Library
Bremerton, WA 98314

1 Long Beach Naval Shipyard
Technical Library (246L)
Long Beach, CA 90801

1 Mare Island Naval Shipyard
Shipyard Technical Library (202.3)
Vallejo, CA 94592

1 Assistant Chief Design Engineer
for Naval Architecture (Code 250)
Mare Island Naval Shipyard
Vallejo, CA 94592

2 U.S. Naval Academy
Annapolis, MD 21402
Attn: Technical Library
Dr. S.A. Elder

1 Naval Postgraduate School
Monterey, CA 93940
Attn: Library (2124)

1 Study Center
National Maritime Research Center
U.S. Merchant Marine Academy
Kings Point, LI, NY 11024

1 The Pennsylvania State University
Applied Research Laboratory (Library)
P.O. Box 30
State College, PA 16801

1 Dr. B. Parkin, Director
Garfield Thomas Water Tunnel
Applied Research Laboratory
P.O. Box 30
State College, PA

1 Bolt, Beranek & Newman (Library)
50 Moulton Street
Cambridge, MA 02138

1 Bethlehem Steel Corporation
25 Broadway
New York, NY 10004
Attn: Library - Shipbuilding

1 Cambridge Acoustical Associates, Inc.
54 Rindge Ave Extension
Cambridge, MA 02140

1 R & D Manager
Electric Boat Division
General Dynamics Corporation
Groton, CT 06340

1 Gibbs & Cox, Inc. (Tech Info Control)
21 West Street
New York, NY 10006

1 Department of Ocean Engineering
University of Hawaii (Library)
2565 The Mall
Honolulu, HI 96822

2 Institute of Hydraulic Research
The University of Iowa
Iowa City, IA 52240
Attn: Library
Dr. L. Landweber

3 Department of Ocean Engineering
Massachusetts Institute of Technology
Cambridge, MA 02139
Attn: Prof. P. Leehey
Prof. J. Newman
Prof. J. Kerwin

1 Engineering Technical Reports
Room 10-500
Massachusetts Institute of Technology
Cambridge, MA 02139

2 St. Anthony Falls Hydraulic Laboratory
University of Minnesota
Mississippi River at 3rd Avenue S.E.
Minneapolis, MN 55414
Attn: Dr. Roger Arndt
Library

2 Department of Naval Architecture
and Marine Engineering - North Campus
University of Michigan
Ann Arbor, MI 48109
Attn: Library
Dr. T. Francis Ogilvie

2 Davidson Laboratory
Stevens Institute of Technology
711 Hudson Street
Hoboken, NJ 07030
Attn: Library
Dr. J. Breslin

2 Stanford University
Stanford, CA 94305
Attn: Engineering Library
Dr. R. Street

1 Webb Institute of Naval Architecture
Attn: Library
Crescent Beach Road
Glen Cove, LI, NY 11542

1 National Science Foundation
Engineering Division Library
1800 G. Street NW
Washington, DC 20550

1 Dr. Douglas E. Humphreys, Code 794
Naval Coastal Systems Laboratory
Panama City, FL 32401